

Species Abundance Distribution and Species Accumulation Curve: A General Framework and Results

Cheuk Ting LI

Department of Information Engineering,

The Chinese University of Hong Kong, Shatin, Hong Kong.

ctli@ie.cuhk.edu.hk

Kim-Hung LI

Asian Cities Research Centre Ltd., Win Plaza,

9 Sheung Hei Street, San Po Kong, Hong Kong.

khli@acrc.hk

April 23, 2022

Abstract

This paper aims at building a general framework that unifies species abundance distribution and species accumulation curve. The framework has two main features. First, the species are modeled as a Poisson process, conditioned on which the individuals are generated by another Poisson process over the time axis. Species-time relationship is explicitly depicted by this doubly stochastic Poisson process. Second, it allows the total number of species to be finite or infinite. As an extreme, we may observe species with zero detection probability. If it happens, there must be an infinite number of such species. Inspired by a diagnostic plot, we propose a special parametric model, where the species abundance distribution is the Engen's extended negative binomial distribution,

and the species accumulation curve encompasses some popular families such as the power law and the hyperbola law. The model can be extended to incorporate species with zero detection probability. We also consider stopping rules other than fixing the observation period. Log-likelihood functions under different scenarios are presented.

Keywords: Engen's extended negative binomial distribution; Good-Toulmin estimator; Power law; Rarefaction curve; Stopping rule; Zero-probability species.

1 Introduction

Understanding the species abundance in an ecological community has long been an important and challenging task for ecologists. Such knowledge is paramount in conservation planning and biodiversity management (Matthews and Whittaker [2015]). An exhaustive species inventory is too labor and resource intensive to be practical. Information about species abundance can thus be acquired mainly through a survey. Formal statistical model appeared in the pioneering work of Fisher (Fisher et al. [1943]) where log-series distribution was recommended. Comprehensive review of the field can be found in McGill et al. [2007] and Matthews and Whittaker [2014].

Let $N = (N_0, N_1, \dots)$ where N_k is the number of species in a community that are represented exactly k times in the survey. We do not observe the whole N , but $\tilde{N} = (N_1, N_2, \dots)$ which is the zero-truncated N . In other words, we do not know how many species are not seen in the survey. We call the vector \tilde{N} , the frequency of frequencies. A typical assumption is that \tilde{N} given $N_+ = \sum_{k=1}^{\infty} N_k$ follows a multinomial distribution, $\text{Multinomial}(N_+, p)$, where $p = (p_1, p_2, \dots)$ is a probability vector, such that p_k is the probability for a randomly selected recorded species to be observed k times in the study. We call this vector p , the species abundance distribution. Vector p is survey-dependent. The data collection method as well as the length of the observation period have effect on p . This dependence complicates the interpretation of p as well as the comparison of results among studies.

Apart from considering the distribution of \tilde{N} , some researchers study the (individual-based) species accumulation curve which delineates the relation between the number

of observed species and the sampling effort. The survey is viewed as a data-collection process in which more and more sampling effort is devoted. Sampling effort can be of continuous type, such as the area of land or the volume of water inspected, or the duration of the survey. Discrete type sampling effort can be the sample size, or the number of trapping occasions. To emphasize the sampling effort considered, the curve is called species-time curve when the sampling effort is time, and species-area curve when area sampled is the sampling effort. Species-area curve has been studied extensively in literature. Review of it can be found in Tjørve [2003, 2009] and Dengler [2009]. In this paper, we use time as the measure of sampling effort. We consider the vector N to be a function of the time t , denoted as $N(t)$. Notations N_k , \tilde{N} , N_+ , p and p_k are likewise denoted as $N_k(t)$, $\tilde{N}(t)$, $N_+(t)$, $p(t)$ and $p_k(t)$ respectively. Because of the great similarity of the species-time relation and species-area relation (Preston [1960], White et al. [2006], Magurran [2007]), time and area are treated as if they are interchangeable in this paper.

Throughout the paper, we denote the time at which the survey starts as time 0, and the time at which the data are summarized and analyzed as time $t_0 > 0$. Therefore, a species abundance distribution is $p(t_0)$ which describes the distribution of the frequency of the seen species.

Standard parametric species accumulation curve approach takes estimation as a curve fitting problem. Linear or non-linear least-squares method is used to fit a parametric curve to the empirical species accumulation curve or the rarefaction curve which is a nonparametric estimate of the expected species accumulation curve. The fitted curve can then be used in interpolation or extrapolation.

There are marked differences between the parametric approaches in the species abundance distribution and the species accumulation curve. The species abundance distribution approach uses the data $\tilde{N}(t_0)$, whereas the species accumulation curve approach uses $\{N_+(t)\}_{0 \leq t \leq t_0}$ or the rarefaction curve. To unify the two approaches, we propose a statistical model on the whole $\{N_k(t)\}_{k \geq 1, 0 \leq t \leq t_0}$.

Apart from unifying species abundance distribution and species accumulation curve, we want the model to be capable for finite or infinite D , the total number of species, or formally the total number of species that will eventually be seen as time approaches in-

finity. In species abundance distribution approach, a common assumption is that D is a finite unknown value. While many ecologists agree with this assumption, the finiteness of D is challenged by significant amount of empirical evidences and application needs. The success of the log-series distribution, which is a species abundance distribution that assumes infinite D , is noteworthy. Furthermore, an ecological system is usually open in the sense that organisms can enter and leave the system at will. It can largely magnify the number of rare species we can observe in the survey. Errors in the identification process can also be a continuous source of rare species. A well-known example is the missequencing in pyrosequencing of DNA. It was found that the probability of missequencing DNA is significant (Dickie [2010], Quince et al. [2011], Abnizova et al. [2017]). An extreme kind of rare species is species with zero detection probability. We call such species, zero-probability species, and all other species, positive-rate species. Zero-probability species can either be seen only once or unseen in the survey. If there are finite number of zero-probability species, the probability of observing any of them is zero. Therefore, if a zero-probability species is observed in the study, it is almost sure that there are infinite number of them.

In this paper, we propose a new sampling process, called the mixed Poisson partition process in Section 2. It can handle the case where D is finite or infinite, and allows existence of zero-probability species. The appearance times of individuals in each species follows a Poisson process which are independent across species. The main idea is to assume the rates of the processes, say $\lambda_1, \lambda_2, \dots$, are again outcomes of a Poisson process. Whether D is finite or not depends on the intensity measure of the latter process. If the intensity measure is finite, D is almost surely finite, and follows a Poisson distribution. Probabilistic properties of $\tilde{N}(t)$ as well as the maximum likelihood estimation are considered in Section 3. In Section 4, we study the expected species accumulation curve. There are two ways to parametrize the mixed Poisson partition process: the expected species accumulation curve (which is a Bernstein function that passes through the origin), and the species abundance distribution together with a scaling factor. In Section 5, we study a graphical tool and its associated family of expected species accumulation curve. The $p(t)$ is the probability vector of the Engen's extended negative binomial distribution in the support $\{1, 2, \dots\}$. The family is then

extended to include zero-probability species. Section 6 is on sampling designs. Stopping rules other than fixing the observation period are considered. We consider an example in Section 7 demonstrating the use of the graphical tool. We give a conclusion in Section 8.

2 Mixed Poisson partition process

In a species richness survey, individuals arrive as a labeled point process, where each point has two attributes: its time of observation, and which one of the (finitely or infinitely many) species it belongs. Let $\mathcal{P}_c(A)$ denote the set of finite or countably infinite subsets of a set A . The species labels induces a partition on the set of individuals, where each subset in the partition contains individuals belonging to the same species. A partitioned point process is a random element G over the space $\mathcal{P}_c(\mathcal{P}_c(\mathbb{R}_{\geq 0}))$, where $\mathbb{R}_{\geq 0}$ stands for the set of all non-negative real numbers. If $G = \{\eta_1, \eta_2, \dots\}$, it means that each $\eta_i \in \mathcal{P}_c(\mathbb{R}_{\geq 0})$ is the set of times at which individuals of species i are observed. Sample G is an unordered set, and the labels i of η_i has no meaning. For example, if there are D species, and the individuals of each species, say species i , are observed independently according to a Poisson process with rate λ_i , then η_i is generated according to a Poisson process with rate λ_i , and $G = \{\eta_1, \dots, \eta_D\}$. It reduces to the mixed Poisson model when we further assume that $\lambda_1, \dots, \lambda_D$ are random sample from a mixing distribution. To incorporate the case where the number of species is infinite, we define the following sampling model:

Definition 1: (Mixed Poisson partition process) *The mixed Poisson partition process is parameterized by a species intensity measure ν , which is a measure over $\mathbb{R}_{\geq 0}$ satisfying*

$$\int_0^\infty \min\{1, \lambda^{-1}\} \nu(d\lambda) < \infty. \quad (1)$$

The definition of mixed Poisson partition process consists of three steps:

1. *(Generation of positive rates of species) Given ν , define $\tilde{\nu}$ to be a measure over $\mathbb{R}_{>0}$ ($\mathbb{R}_{>0}$ is the set of positive real numbers) by*

$$\tilde{\nu}(d\lambda) = \frac{1}{\lambda} \nu(d\lambda),$$

i.e., $d\tilde{\nu}/d\nu = 1/\lambda$ for $\lambda > 0$. Generate $\lambda_1, \lambda_2, \dots$ (a finite or countably infinite sequence) according to a Poisson process with intensity measure $\tilde{\nu}$.

2. (Generation of individuals of positive-rate species) For each λ_i in Step 1, we generate $\eta_i \in \mathcal{P}_c(\mathbb{R}_{\geq 0})$ (independent across i) according to a Poisson process with rate λ_i .
3. (Generation of individuals of zero-probability species) We generate $\eta_0 \in \mathcal{P}_c(\mathbb{R}_{\geq 0})$ according to a Poisson process with rate $\nu(\{0\})$, independent of η_1, η_2, \dots . This represents the times of appearance for all the zero-probability species.

Finally, we take $G = \{\eta_1, \eta_2, \dots\} \cup \eta_0$. For any $i \geq 1$, all points in η_i are from the same species, whereas each point in η_0 is from a different species (we use a slight abuse of notation to treat each point in η_0 as a point process with only one point).

Similar to Step 1, Zhou et al. [2017] also considers the species to be generated according to a random process. However, their model does not involve time, and hence does not describe the species accumulation curve. Although their model includes cases where D is infinite, it fails to handle zero-probability species.

Measures ν and $\tilde{\nu}$ may be finite or infinite. As the expected number of individuals seen in time interval $[0, t]$ is equal to $t\nu(\mathbb{R}_{\geq 0})$ (see (5) in Section 3), the finiteness of ν means that this expected value is finite for any finite t . If $\tilde{\nu}$ is finite, the expected number of positive-rate species in the community is finite. From Step 3 in the definition, if $\nu(\{0\}) > 0$, there are infinite number of zero-probability species and they arrive at a constant rate. With probability one, D is finite if and only if $\nu(\{0\}) = 0$ and $\tilde{\nu}(\mathbb{R}_{>0}) = \int_0^\infty (1/\lambda)\nu(d\lambda) < \infty$ (see (6) in Section 3). In such case, D follows a Poisson distribution with mean $\int_0^\infty (1/\lambda)\nu(d\lambda)$, which we denote as $D \sim \text{Poi}(\int_0^\infty (1/\lambda)\nu(d\lambda))$. Measure $\tilde{\nu}$ models the rate of a randomly selected positive-rate species in the community, whilst ν is its size-biased version which models the rate (including the zero-probability species) of the species to which a randomly selected observed *individual* belongs. Condition (1) is essential because it is equivalent to $E(N_+(t)) < \infty$ for any finite non-negative t as will be proved in Section 3. Figure 1 illustrates the generation of the mixed Poisson partition process.

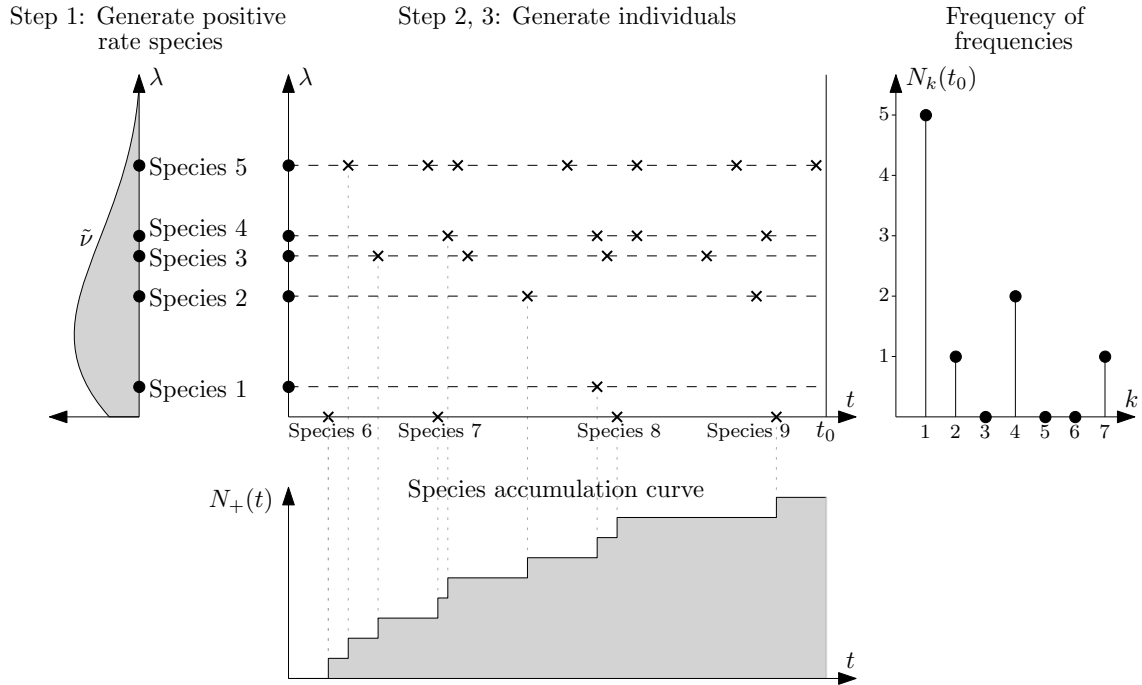


Figure 1: An illustration of the mixed Poisson partition process. In step 1, we generate the rates λ_i of the positive-rate species according to a Poisson process with intensity measure $\tilde{\nu}$. If $\tilde{\nu}(\mathbb{R}_{>0}) < \infty$, then this is equivalent to first generating n_{pos} , the number of positive-rate species according to $\text{Poi}(\tilde{\nu}(\mathbb{R}_{>0}))$, and then generating a random sample $\lambda_1, \dots, \lambda_{n_{pos}}$ of size n_{pos} from the probability measure $\tilde{\nu}/\tilde{\nu}(\mathbb{R}_{>0})$. In step 2, we generate the individuals of species i according to a Poisson process with rate λ_i for $i = 1, \dots, n_{pos}$. In step 3, we generate the individuals of zero-probability species (species 6 to 9 in the figure) according to a Poisson process with rate $\nu(\{0\})$.

The specification of ν is equivalent to $\tilde{\nu}$ and $\nu(\{0\})$ as a whole. The following alternative equivalent definition unifies the three steps in the definition into one. Proof of the equivalence of the two definitions is given in Appendix A.

Definition 2: (Equivalent definition of mixed Poisson partition process)

Given a measure ν , define $\mathring{\nu}$ to be a measure over $\mathbb{R}_{\geq 0}^2$ by

$$\mathring{\nu}(A) = \int \int_0^\infty \mathbf{1}\{(\lambda, t) \in A\} e^{-\lambda t} dt \cdot \nu(d\lambda)$$

for any measurable set $A \subseteq \mathbb{R}_{\geq 0}^2$ where $\mathbf{1}\{.\}$ is the indicator function. Generate $(\lambda_1, t_1), (\lambda_2, t_2), \dots$ (a finite or countably infinite sequence) according to a Poisson process with intensity measure $\mathring{\nu}$. For each simulated (λ_i, t_i) , we generate η_i (independent across i) according to a Poisson process with rate λ_i , conditioned on the event that the first point is at time t_i . (That is, it contains the point t_i together with a Poisson process starting at time t_i . If $\lambda_i = 0$, then η_i contains only one point t_i .) Finally, we take $G = \{\eta_1, \eta_2, \dots\}$.

Definition 2 models the species that will eventually be observed in the study. The first appearance time for each of such species (i.e. the first point of each η_i) is explicitly included in the definition of $\mathring{\nu}$.

3 Frequency of frequencies and maximum likelihood estimation

A common form of species abundance data is $\tilde{N}(t)$. Understanding the probabilistic properties of it is essential. Let $\lambda_1, \lambda_2, \dots$ be the values drawn from the Poisson process with intensity measure $\tilde{\nu}$. For each λ , it contributes to one of the counts $N_k(t)$, where k follows a Poisson distribution $\text{Poi}(\lambda t)$. By the splitting property of Poisson process, their total contribution to $N_k(t)$ follows $\text{Poi}\left(\int (\lambda t)^k (k!)^{-1} e^{-\lambda t} \tilde{\nu}(d\lambda)\right)$ distribution independent across k . For the contribution of $\nu(\{0\})$ to $N_k(t)$, η_0 is a Poisson process with rate $\nu(\{0\})$. It affects only $N_1(t)$ by increasing its value by a random variable with

distribution $\text{Poi}(\nu(\{0\})t)$. Therefore,

$$N_k(t) \sim \text{Poi} \left(\int \frac{(\lambda t)^k e^{-\lambda t}}{k!} \tilde{\nu}(d\lambda) + \mathbf{1}\{k=1\} \nu(\{0\})t \right) = \text{Poi} \left(\int \frac{\lambda^{k-1} t^k e^{-\lambda t}}{k!} \nu(d\lambda) \right), \quad (2)$$

with the convention $0^0 = 1$. As $N_+(t) = \sum_{k=1}^{\infty} N_k(t)$ and all $\{N_k(t)\}$ are independent,

$$N_+(t) \sim \text{Poi} \left(\sum_{k=1}^{\infty} \int \frac{\lambda^{k-1} t^k e^{-\lambda t}}{k!} \nu(d\lambda) \right) = \text{Poi} \left(\int \frac{1 - e^{-\lambda t}}{\lambda} \nu(d\lambda) \right), \quad (3)$$

where we assume $(1 - e^{-\lambda t})/\lambda = t$ when $\lambda = 0$. From (2) and (3),

$$E(N_k(t)) = \int \frac{\lambda^{k-1} t^k e^{-\lambda t}}{k!} \nu(d\lambda), \quad \text{for } k \geq 1, \quad \text{and} \quad E(N_+(t)) = \int \frac{1 - e^{-\lambda t}}{\lambda} \nu(d\lambda). \quad (4)$$

Condition (1) is equivalent to $E(N_+(t)) < \infty$ for any finite non-negative t because under Condition (1),

$$\int \frac{1 - e^{-\lambda t}}{\lambda} \nu(d\lambda) \leq \int \min\{t, \lambda^{-1}\} \nu(d\lambda) \leq \max\{t, 1\} \int \min\{1, \lambda^{-1}\} \nu(d\lambda) < \infty$$

for any finite non-negative t , and if $E(N_+(1)) < \infty$, then

$$\int \min\{1, \lambda^{-1}\} \nu(d\lambda) \leq \frac{1}{1 - e^{-1}} \int \frac{1 - e^{-\lambda}}{\lambda} \nu(d\lambda) = \frac{E(N_+(1))}{1 - e^{-1}} < \infty.$$

Let $S(t) = \sum_{k=1}^{\infty} k N_k(t)$ be the number of individuals observed before time t . Then

$$E(S(t)) = \sum_{k=1}^{\infty} k \int \frac{\lambda^{k-1} t^k e^{-\lambda t}}{k!} \nu(d\lambda) = t \int \nu(d\lambda). \quad (5)$$

Furthermore,

$$E(D) = \lim_{t \rightarrow \infty} E(N_+(t)) = \lim_{t \rightarrow \infty} \int \frac{1 - e^{-\lambda t}}{\lambda} \nu(d\lambda) = \begin{cases} \infty & (\nu(\{0\}) > 0) \\ \int \tilde{\nu}(d\lambda) & (\nu(\{0\}) = 0). \end{cases} \quad (6)$$

The multinomial model in Section 1 remains valid under the framework, and

$$p_k(t) = \frac{E(N_k(t))}{E(N_+(t))} = \frac{\int (k!)^{-1} \lambda^{k-1} t^k e^{-\lambda t} \nu(d\lambda)}{\int \lambda^{-1} (1 - e^{-\lambda t}) \nu(d\lambda)} \quad (k = 1, 2, \dots). \quad (7)$$

If $E(D)$ is finite, the frequency of each species will keep increasing without limit, and $\lim_{t \rightarrow \infty} p_k(t) = 0$ for any fixed k .

Let $n_k(t_0)$ be the observed $N_k(t_0)$ for $k = 1, 2, \dots$ and $\tilde{n}(t_0) = \{n_k(t_0)\}_{k \geq 1}$. From (2), the joint probability mass function of $\tilde{N}(t_0)$ is

$$pr(\tilde{N}(t_0) = \tilde{n}(t_0) \mid \nu) = \exp(-E(N_+(t_0))) \prod_{k=1}^{\infty} \frac{(E(N_k(t_0)))^{n_k(t_0)}}{n_k(t_0)!}.$$

In terms of the expected frequency of frequencies, the log-likelihood function is

$$\log(\mathcal{L}(\nu | \tilde{n}(t_0))) = -E(N_+(t_0)) + \sum_{k=1}^{\infty} n_k(t_0) \log(E(N_k(t_0))). \quad (8)$$

In terms of $p(t_0)$ and $E(N_+(t_0))$, it is

$$\log(\mathcal{L}(\nu | \tilde{n}(t_0))) = -E(N_+(t_0)) + n_+(t_0) \log(E(N_+(t_0))) + \sum_{k=1}^{\infty} n_k(t_0) \log(p_k(t_0)).$$

If $p(t_0)$ and $E(N_+(t_0))$ are independent, the maximum likelihood estimator of $p(t_0)$ is the conditional maximum likelihood estimator (conditional on the observed $n_+(t_0)$) of the multinomial distribution, $Multinomial(n_+(t_0), p(t_0))$ in Section 1. The maximum likelihood estimator of $E(N_+(t_0))$ is $n_+(t_0)$, i.e. the maximum likelihood estimate of the expected number of seen species is equal to the observed number of seen species.

Remark 1: When there are zero-probability species, the probability vector, $p(t)$ is a weighted average of two probability vectors, one for the zero-probability species and one for the positive-rate species,

$$p_k(t) = (1 - \alpha(t))\mathbf{1}\{k = 1\} + \alpha(t)q_k(t), \quad (k = 1, 2, \dots)$$

where

$$\alpha(t) = \frac{\int(1 - e^{-\lambda t})\tilde{\nu}(d\lambda)}{\nu(\{0\})t + \int(1 - e^{-\lambda t})\tilde{\nu}(d\lambda)}$$

is the relative weight for the positive-rate species, and

$$q_k(t) = \frac{\int(k!)^{-1}(\lambda t)^k e^{-\lambda t}\tilde{\nu}(d\lambda)}{\int(1 - e^{-\lambda t})\tilde{\nu}(d\lambda)}$$

is the probability for a recorded positive-rate species in time $[0, t]$ to have frequency k in time $[0, t]$. The log-likelihood function can be re-expressed as

$$\begin{aligned} \log(\mathcal{L}(\nu | \tilde{n}(t_0))) &= -E(N_+(t_0)) + n_+(t_0) \log(E(N_+(t_0))) + (n_+(t_0) - n_1(t_0)) \log(\alpha(t_0)) \\ &\quad + \sum_{k=2}^{\infty} n_k(t_0) \log(q_k(t_0)) + n_1(t_0) \log(1 - \alpha(t_0)(1 - q_1(t_0))). \end{aligned}$$

Suppose $E(N_+(t_0))$, $\alpha(t_0)$ and $q(t_0) = (q_1(t_0), q_2(t_0), \dots)$ are independent parameters. From the partial derivative of the log-likelihood function with respect to $\alpha(t_0)$, we know that the log-likelihood function is increasing in $\alpha(t_0)$ when $\alpha(t_0) \leq h(q(t_0))$, and decreasing when $\alpha(t_0) \geq h(q(t_0))$, where

$$h(q(t_0)) = \frac{n_+(t_0) - n_1(t_0)}{n_+(t_0)(1 - q_1(t_0))}.$$

Hence, the optimal $\alpha(t_0)$ (for fixed $q(t_0)$) is $\min\{h(q(t_0)), 1\}$. It means that if the projected singleton count from the positive-rate species is larger than or equal to the observed singleton count (i.e. $n_+(t_0)q_1(t_0) \geq n_1(t_0)$), then $\alpha(t_0) = 1$. The maximum likelihood estimate of $q(t_0)$, denoted as $\hat{q}(t_0)$, is the value that maximizes

$$(n_+(t_0) - n_1(t_0)) \log(\min\{h(\hat{q}(t_0)), 1\}) + \sum_{k=2}^{\infty} n_k(t_0) \log(q_k(t_0)) \\ + n_1(t_0) \log(1 - \min\{h(\hat{q}(t_0)), 1\}(1 - q_1(t_0))),$$

and that of α is $\hat{\alpha} = \min\{h(\hat{q}(t_0)), 1\}$. The maximum likelihood estimator of $E(N_+(t_0))$ is $\hat{E}(N_+(t_0)) = n_+(t_0)$, i.e. the maximum likelihood estimate of the expected number of seen species is equal to the observed number of seen species. With the above technique, we can reduce the dimensionality of the optimization problem in finding the maximum likelihood estimate.

4 Expected species accumulation curve

Consider the (individual-based) species accumulation curve, which in this paper is $\{N_+(t)\}_{t \geq 0}$. We define the expected species accumulation curve as $\psi(t) = E(N_+(t))$. Equation (4) implies that

$$\psi(t) = \int \frac{1 - e^{-\lambda t}}{\lambda} \nu(d\lambda) = \nu(\{0\})t + \int (1 - e^{-\lambda t}) \tilde{\nu}(d\lambda). \quad (9)$$

Hence, for $k \geq 1$,

$$\psi^{(k)}(t) = \int (-\lambda)^{k-1} e^{-\lambda t} \nu(d\lambda), \quad (10)$$

where $g^{(m)}(t)$ stands for the m -order derivative of function $g(t)$.

From (10), $\psi(t)$ is a Bernstein function (Bernstein [1929], Schilling et al. [2012]) (a function $g(t)$ is a Bernstein function if it is a non-negative real-valued function on $[0, \infty)$ such that $(-1)^k g^{(k)}(t) \leq 0$ for all $k \geq 1$). In considering a restricted model, Boneh et al. [1998] found that $(-1)^{k+1} \psi^{(k)}(t) \geq 0$ and called it, alternating copositivity. Every Bernstein function $g(t)$ with $g(0) = 0$ has a unique Lévy-Khintchine representation

$$g(t) = \tau t + \int_0^\infty (1 - e^{-\lambda t}) \mu(d\lambda), \quad (11)$$

where $\tau \geq 0$, and μ is a measure over $[0, \infty)$ such that $\int_0^\infty \min\{1, \lambda\} \mu(d\lambda) < \infty$. For $\psi(t)$, by comparing (9) and (11), we have $\tau = \nu(\{0\})$ and $\mu = \tilde{\nu}$. The condition

$\int_0^\infty \min\{1, \lambda\} \mu(d\lambda) < \infty$ is equivalent to Condition (1). Hence, there is a one-to-one correspondence between a Bernstein function $\psi(t)$ with $\psi(0) = 0$ and ν (or $\nu(\{0\})$) and $\tilde{\nu}$ as a whole).

From (4) and (10), for $k = 1, 2, \dots$

$$\psi^{(k)}(t) = (-1)^{k+1} \frac{k!}{t^k} E(N_k(t)). \quad (12)$$

It is worth pointing out that analogous expression for (12) appears in Béguinot [2016] as an approximate formula under the multinomial model for fixed total number of observed individuals with the expected species accumulation curve being a function of sample size instead of time, and the derivative operator replaced by the difference operator. From (8), the log-likelihood function can be re-expressed as

$$\log(\mathcal{L}(\psi \mid \tilde{n}(t_0))) = -\psi(t_0) + \sum_{k=1}^{\infty} n_k(t_0) \log(|\psi^{(k)}(t_0)|).$$

Let us consider the power expansion of $\psi(t)$.

$$\begin{aligned} \psi(t) &= \int \frac{1 - e^{-\lambda t_0}}{\lambda} \nu(d\lambda) - \int \frac{(e^{\lambda(t_0-t)} - 1)e^{-\lambda t_0}}{\lambda} \nu(d\lambda) \\ &= E(N_+(t_0)) + \sum_{k=1}^{\infty} (-1)^{k+1} E(N_k(t_0)) \left(\frac{t}{t_0} - 1 \right)^k. \end{aligned} \quad (13)$$

Equation (13) can be re-expressed as

$$\psi(t) = E(N_+(t_0)) \left(1 - \sum_{k=1}^{\infty} p_k(t_0) \left(1 - \frac{t}{t_0} \right)^k \right), \quad (14)$$

where $E(N_+(t_0))$ works as a scale factor. Equations (7), (11), and (14) establishes the one-to-one correspondence between the following three parametrizations of the mixed Poisson partition process: the species intensity measure ν , the expected species accumulation curve $\psi(t)$, and the species abundance distribution $p(t_0)$ in the form of (7) together with $E(N_+(t_0))$ at any fixed t_0 . Equation (13) also implies that the Good-Toulmin estimator (Good and Toulmin [1956])

$$\hat{\psi}(t) = n_+(t_0) + \sum_{k=1}^{\infty} (-1)^{k+1} n_k(t_0) \left(\frac{t}{t_0} - 1 \right)^k$$

remains to be an unbiased estimator of $\psi(t)$ under the framework. This estimator does not perform well when t is large compared to t_0 . However, the estimator works

well in interpolation, and performs satisfactorily in short-term extrapolation when $t_0 < t \leq 2t_0$. The curve $\hat{\psi}(t)$ for $0 \leq t \leq t_0$ is known as the rarefaction curve or randomized species accumulation curve (see for example Colwell et al. [2012]). Good-Toulmin estimator can be re-expressed as $\hat{\psi}(t) = \sum_{k=1}^{\infty} n_k(t_0)(1 - (1 - t/t_0)^k)$ which is more intuitive when $0 \leq t \leq t_0$ because each species with frequency k at time t_0 has probability $(1 - (1 - t/t_0)^k)$ to be observed before time t (Arrhenius [1921]). All derivatives of the rarefaction curve have the correct sign as a Bernstein function for $t \in [0, t_0]$.

We can deduce estimator for the derivative of $\psi(t)$ from the rarefaction curve. For example,

$$\hat{\psi}^{(1)}(t) = \frac{1}{t_0} \sum_{k=1}^{\infty} k n_k(t_0) \left(1 - \frac{t}{t_0}\right)^{k-1}, \quad (15)$$

$$\hat{\psi}^{(2)}(t) = -\frac{1}{t_0^2} \sum_{k=2}^{\infty} k(k-1) n_k(t_0) \left(1 - \frac{t}{t_0}\right)^{k-2}, \quad (16)$$

and

$$\hat{\psi}^{(3)}(t) = \frac{1}{t_0^3} \sum_{k=3}^{\infty} k(k-1)(k-2) n_k(t_0) \left(1 - \frac{t}{t_0}\right)^{k-3}. \quad (17)$$

Function $\hat{\psi}^{(1)}(t)$ which delineates the increasing rate of recorded species is informative. We can draw $1/\hat{\psi}^{(1)}(t)$ as a function of $t \in [0, t_0]$ for $\hat{\psi}^{(1)}(t)$ in (15). We call it, 1/D1 plot. A concave downward curve in the plot is an indication that $E(D) = \infty$. To see the reason, suppose there is a linear function $b + ct$ with positive b and c such that $b + ct \geq 1/\hat{\psi}^{(1)}(t)$ for all $t \geq 0$. Then

$$\psi(t) = \int_0^t \psi^{(1)}(x) dx \geq \int_0^t (b + cx)^{-1} dx = \frac{1}{c} \log \left(1 + \frac{c}{b} t\right).$$

Clearly $E(D) = \lim_{t \rightarrow \infty} \psi(t) = \infty$. If $1/\psi^{(1)}(t)$ is concave downward in $t \in [0, t_0]$, there are many linear functions that bound $1/\psi^{(1)}(t)$ from above for $t \in [0, t_0]$. If $1/\psi^{(1)}(t)$ is bounded by any of these linear functions in the positive half line, $E(D) = \infty$. Therefore, downward concavity of $1/\hat{\psi}^{(1)}(t)$ can be viewed as an indication of $E(D) = \infty$. See also the relation of the 1/D1 plot with the log-series distribution in Section 5.1.

5 Linear derivative ratio family for expected species accumulation curve

5.1 First linear derivative ratio family for expected species accumulation curve

We call a family of expected species accumulation curve, j th linear derivative ratio family, denoted as \mathcal{F}_j , if $-\psi^{(j)}(t)/\psi^{(j+1)}(t)$ is a linear function of t . It can be shown that $\mathcal{F}_1 \subset \mathcal{F}_2 = \mathcal{F}_3 = \dots$ (proof is given in Appendix B). Therefore, we only need to consider \mathcal{F}_1 and \mathcal{F}_2 .

An expected species accumulation curve, $\psi(t)$ belongs to \mathcal{F}_1 if $-\psi^{(1)}(t)/\psi^{(2)}(t) = b + ct$ for some b and c . As $-\psi^{(1)}(t)/\psi^{(2)}(t)$ is non-negative for all $t > 0$, b and c should be non-negative. If $b = 0$, c must be larger than 1, otherwise $\psi(t)$ can be infinite for finite t as seen from (18). This family has a simple diagnostic plot: Draw $-\hat{\psi}^{(1)}(t)/\hat{\psi}^{(2)}(t)$ as a function of $t \in [0, t_0]$ for $\hat{\psi}^{(1)}(t)$ and $\hat{\psi}^{(2)}(t)$ defined in (15) and (16) respectively. If the curve is almost linear, \mathcal{F}_1 is an appropriate model and approximate value of b and c can be obtained from a fitted linear function to the curve. We call the plot, D1/D2 plot.

To find the maximum likelihood estimate, we need the expression for $\psi(t)$ and $\psi^{(k)}(t)$. Fixing $\psi^{(1)}(1) = a > 0$, we have

$$\psi(t) = \begin{cases} \frac{a(b+c)}{c-1} \left(\left(\frac{b+ct}{b+c} \right)^{1-1/c} - \left(\frac{b}{b+c} \right)^{1-1/c} \right) & (c \neq 0, 1), \\ ab \exp(1/b)(1 - \exp(-t/b)) & (c = 0), \\ a(b+1) \log(1 + (t/b)) & (c = 1). \end{cases} \quad (18)$$

Parameter a is a scale parameter. It can be shown that for $k \geq 1$,

$$\psi^{(k)}(t) = \begin{cases} (-1)^{k+1} \frac{a(b+c)^{1-k} c^{k-1} \Gamma(1/c+k-1)}{\Gamma(1/c)} \left(\frac{b+ct}{b+c} \right)^{1-1/c-k} & (c > 0), \\ (-1)^{k+1} ab^{1-k} \exp((1-t)/b) & (c = 0). \end{cases} \quad (19)$$

Clearly $\psi(t)$ in (18) is a Bernstein function that passes through the origin. We can find $E(N_k(t))$ from (19) and (12). It can be shown that $\nu(\{0\}) = 0$, and $\tilde{\nu}$ is

$$\tilde{\nu}(d\lambda) = \begin{cases} \frac{a((b+c)/c)^{1/c} \lambda^{1/c-2}}{\Gamma(1/c)} \exp(-b\lambda/c) d\lambda & (c > 0), \\ ab \exp(1/b) \delta_{1/b}(d\lambda) & (c = 0), \end{cases}$$

where $\delta_{1/b}(A) = \mathbf{1}\{1/b \in A\}$ is the Dirac measure. The expected total number of species is

$$E(D) = \lim_{t \rightarrow \infty} \psi(t) = \begin{cases} a(b+c)^{1/c} b^{1-1/c} (1-c)^{-1} & (0 < c < 1), \\ ab \exp(1/b) & (c = 0), \\ \infty & (c \geq 1). \end{cases}$$

The intensity function $\tilde{\nu}$ takes the form as a gamma distribution with extended shape parameter $1/c - 1$ for non-negative c . Therefore, $p(t)$ is the Engen's extended negative binomial distribution (Engen [1974]) with support $\{1, 2, \dots\}$. We remark that Engen's extended negative binomial distribution also appears in the model studied by Zhou et al. [2017].

For $\psi \in \mathcal{F}_1$, $E(D) = \infty$ if and only if $E(N_k(t))$ keeps increasing as t increases for any fixed k . When $E(D) < \infty$, $E(N_k(t))$ is unimodal with respect to t .

Model \mathcal{F}_1 includes the following existing models:

- Case $c = 0$: Zero-truncated Poisson distribution for species abundance distribution, negative exponential law for expected species accumulation curve.

When $c = 0$, $E(N_k(t)) = ab \exp(1/b)(t/b)^k \exp(-t/b)/k!$ is proportional to a zero-truncated Poisson distribution. All species have the same rate $1/b$. The expected species accumulation curve is $\psi(t) = ab \exp(1/b)(1 - \exp(-t/b))$ which is the negative exponential law. A plot specially designed for the zero-truncated Poisson distribution is to plot $\log(\hat{\psi}^{(1)}(t))$ against $t \in [0, t_0]$. If the model is correct, we should see a curve close to a straight line because $\log(\hat{\psi}^{(1)}(t)) = 1/b + \log(a) - t/b$.

- Case $0 < c < 1$: Zero-truncated negative binomial distribution for species abundance distribution.

When $0 < c < 1$, $\tilde{\nu}$ is proportional to a gamma probability measure, and $p(t)$ is the probability vector for the zero-truncated negative binomial distribution.

- Case $c = 1/2$: Geometric distribution for species abundance distribution, hyperbola law for expected species accumulation curve.

The case $c = 1/2$ is a special case of the previous case. Measure $\tilde{\nu}$ is proportional to the exponential probability measure and $p(t)$ is a geometric probability vector.

The expected species accumulation curve is $\psi(t) = a(2b+1)^2t/(2b(t+2b))$ which is the hyperbola law (also known as Michaelis-Menten equation and Monod model). A plot specially designed for geometric distribution is to plot $(\hat{\psi}^{(1)}(t))^{-1/2}$ as a function of $t \in [0, t_0]$. If geometric distribution fits the data, we should see an almost linear curve because $(\psi^{(1)}(t))^{-1/2} = (t + 2b)/(a^{1/2}(2b + 1))$.

- Case $c = 1$: Log-series distribution for species abundance distribution, Kobayashi's logarithm law for expected species accumulation curve.

When $c = 1$, $E(N_k(t)) = a(b+1)(t/(t+b))^k/k$ corresponding to the log-series distribution. The expected species accumulation curve is $\psi(t) = a(b+1) \log(1+t/b)$ which was introduced in Kobayashi [1975] (see also Fisher et al. [1943] and May [1975]). A graph for the log-series distribution is to draw $1/\hat{\psi}^{(1)}(t)$ as a function of t (it is the 1/D1 plot in Section 4; the curve in 1/D1 plot is concave downward when the data have more rare species than what the log-series distribution can explain). If the model is good, the curve should be close to a straight line because $1/\psi^{(1)}(t) = (b+t)/(a(b+1))$.

- Case $c > 1$ and $b = 0$: Power law for expected species accumulation curve.

When $c > 1$ and $b = 0$, $\psi(t) = act^{1-1/c}/(c-1)$ is the power law. The k th element of $p(t)$ is

$$p_k(t) = \frac{(c-1)\Gamma(1/c+k-1)}{k!c\Gamma(1/c)} \quad (k = 1, 2, \dots), \quad (20)$$

which does not depend on t . It is proved in Appendix C that this is the only $p(t)$ which is invariant to t . For any $\psi \in \mathcal{F}_1$ with $c > 1$, $\lim_{t \rightarrow \infty} p(t)$ is a probability vector in (20). A simple graph to check the power law is to plot $\log(\hat{\psi}^{(1)}(t))$ against $\log(t)$. The curve should be approximately linear because $\log(\psi^{(1)}(t)) = \log(a) - c^{-1} \log(t)$. We call this plot, log(D)-log plot. Currently the standard diagnostic plot for power law is the log-log plot, which plots $\log(\psi(t))$ against $\log(t)$. It is easy to compare the performance of the log-log plot and the log(D)-log plot without using any data. Draw the two plots for $\psi(t) = \log(1+wt)$, which is the expected species accumulation curve for a log-series model (i.e. plotting $\log(\log(1+wt))$ against $\log(t)$, and plotting $\log(w/(1+wt))$ against $\log(t)$) for various values of w . We will see how well log(D)-log plot outperforms log-log plot.

In May [1975], $\log(\psi(t)) \approx b + c \log(t)$ is viewed as a general observed pattern for lognormal distribution as well as some other species abundance distributions. When c approaches infinity, $\psi(t)$ tends to at which corresponds to the case when all species have zero detection probability.

5.2 Second linear derivative ratio family of expected species accumulation curve

An expected species accumulation curve, $\psi(t)$ belongs to \mathcal{F}_2 if $-\psi^{(2)}(t)/\psi^{(3)}(t) = \tilde{b} + \tilde{c}t$. To investigate how well \mathcal{F}_2 fits a data, we can plot the function $-\hat{\psi}^{(2)}(t)/\hat{\psi}^{(3)}(t)$ for $t \in [0, t_0]$ where $\hat{\psi}^{(2)}(t)$ and $\hat{\psi}^{(3)}(t)$ are defined in (16) and (17) respectively. A linear pattern in the plot indicates the model fits the data, and the intercept and slope of an approximate straight line provide estimates of \tilde{b} and \tilde{c} respectively. We call the plot, D2/D3 plot.

There is close relation between the $\psi(t)$ for the first and second linear derivative ratio families. For the second linear derivative ratio family, if we fix $\psi^{(2)}(1) = -\tilde{a}$ and $\psi^{(1)}(1) = \tilde{r} + \tilde{a}(\tilde{b} + \tilde{c})/(1 - \tilde{c})$, it can be proved that

$$\mathcal{F}_2(t \mid \tilde{a}, \tilde{b}, \tilde{c}, \tilde{r}) = \tilde{r}t + \mathcal{F}_1\left(t \mid \tilde{a}(\tilde{b} + \tilde{c})/(1 - \tilde{c}), \tilde{b}/(1 - \tilde{c}), \tilde{c}/(1 - \tilde{c})\right),$$

where $\mathcal{F}_2(t \mid \tilde{a}, \tilde{b}, \tilde{c}, \tilde{r})$ denotes the $\psi(t)$ for the second linear derivative ratio family, and $\mathcal{F}_1(t \mid a, b, c)$ denotes the $\psi(t)$ for the first linear derivative ratio family. We have $\tilde{a} > 0$, $\tilde{b} \geq 0$, $0 \leq \tilde{c} < 1$, and $\tilde{r} \geq 0$. Furthermore, if $\tilde{b} = 0$, then $1/2 < \tilde{c} < 1$, otherwise $\psi(t)$ will be infinite for finite t . The linear component $\tilde{r}t$ in $\mathcal{F}_2(t \mid \tilde{a}, \tilde{b}, \tilde{c}, \tilde{r})$ is the part for the zero-probability species. Therefore, \mathcal{F}_2 is nothing but a mixture of zero-probability species and \mathcal{F}_1 . If $n_1(t_0)$ is large, and an approximate linear curve appears in D2/D3 plot but not in D1/D2 plot, it is a hint that $\nu(\{0\})$ may be positive.

6 Sampling design

When a survey is viewed as a data collection process, there should be a stopping rule to determine when to stop. In the preceding sections, we consider a simple stopping rule – stop the study at a predesignated time t_0 . This design has two weaknesses.

First, it does not control directly the amount of information collected because the size of our data is a random variable, the distribution of which we may have limited knowledge before the study. Second, it collects all available information within the survey period, instead of focusing on the most valuable information and ignoring some minor information in order to save labor.

For the first weakness, we may stop the survey as soon as a fixed number of species are recorded. To ensure termination of study with probability one, we set an upper bound for the study period which is the time at which the data collection process must end. The stopping rule principle states that the likelihood function is the same irrespective of the stopping rule (Raiffa and Schlaifer [1961], Berger and Berry [1988]). By this principle, the likelihood function of the proposed design is identical to the one with the actual stopping time pretended to be fixed instead of random. In other words, the log-likelihood function in (8) can be used with t_0 being the realization of the random stopping time.

For the second weakness, we can halt recording a species as soon as its frequency reaches a fixed positive integer, say ρ . Thus the observation period for each species varies. The period is short for common species, and long for rare species. Again, we need to set an upper bound for the study period, say t_0 for all species. We call this design, the ρ -appearance design. This design places more emphasis on rare species than common species which is in line with the common understanding that information about the rare species is critical in biodiversity estimation. In bird survey, species can be identified by distant sightings or short bursts of song. Stop recording common species early helps the researcher concentrating more on the rare species. When $\rho = \infty$, we obtain $\tilde{n}(t_0)$. When $\rho = 1$, we record only the first appearance-time of each seen species. It is exactly the information available in the empirical species accumulation curve.

In this design, we collect value (R_i, J_i) for each seen species, say species i . Species i has observed frequency J_i at time R_i . Clearly $R_i \leq t_0$ for all i . Suppose we call the species with observed frequency less than ρ as rare species, and all other species as common species. For rare species, $(R_i, J_i) = (t_0, J_i)$ where J_i is the frequency of species i in the whole study period $[0, t_0]$. No information is lost for rare species. For common

species, $(R_i, J_i) = (R_i, \rho)$ where R_i is the appearance time of the ρ th individual of species i . We call R_i , the ρ -appearance time of species i . We do not know the actual frequency of common species in $[0, t_0]$. The values $n_1(t_0), \dots, n_{\rho-1}(t_0)$ and $n_+(t_0)$ are still available. It is proved in Appendix D that the log-likelihood function given a realization of $\{(R_i, J_i)\}_i$, say $\{(r_i, j_i)\}_i$ is

$$\log(\mathcal{L}(\nu | \{r_i, j_i\}_i)) = -\psi(t_0) + \sum_{j=1}^{\rho-1} n_j(t_0) \log(|\psi^{(j)}(t_0)|) + \sum_{r_i < t_0} \log(|\psi^{(\rho)}(r_i)|). \quad (21)$$

The above log-likelihood function can also be obtained from the stopping rule principle. As the likelihood function depends only on the data, but not the stopping rule, the likelihood can be found by pretending that r_i is fixed to the observed value and j_i is random for each i . Equation (21) is the log-likelihood function of this latter artificial design (see (22) for the relation between $\psi^{(\rho)}(r)$ and the intensity function of the ρ -appearance time). A computational advantage of ρ -appearance design is that the log-likelihood function is easy to calculate even for complicated $\psi(t)$ because it requires only the leading ρ derivatives of $\psi(t)$.

The case when $\rho = 1$ is of interest. We observe the 1-appearance time of each seen species. It is the information of the empirical species accumulation curve. The log-likelihood function is

$$\log(\mathcal{L}(\nu | \{r_i, j_i\}_i)) = -\psi(t_0) + \sum_i \log(\psi^{(1)}(r_i)).$$

Two differences between the maximum likelihood estimate approach and the curve fitting method for the empirical species accumulation curve are noteworthy. First, similar to the result in Section 3, the maximum likelihood estimate of $\psi(t_0)$ ($= E(N_+(t_0))$) is usually equal to $n_+(t_0)$ and it is not the case in the curve fitting approach. Second, maximum likelihood estimate approach fits $\psi^{(1)}(t)$ to the 1-appearance times. Standard curve fitting approach fits $\psi(t)$ to the empirical species accumulation curve. By the displacement theorem of Poisson process (Kingman [1993]), the ρ -appearance times r 's form a Poisson process with intensity function

$$\int \frac{\lambda^\rho r^{\rho-1} e^{-\lambda r}}{(\rho-1)!} \tilde{\nu}(d\lambda) = \int \frac{(\lambda r)^{\rho-1} e^{-\lambda r}}{(\rho-1)!} \nu(d\lambda) = \frac{r^{\rho-1}}{(\rho-1)!} (-1)^{\rho-1} \psi^{(\rho)}(r). \quad (22)$$

Therefore, $\psi^{(1)}(t)$ is the intensity function of the 1-appearance times. The maximum

Table 1. Swine feces data and estimates of $E(N_k(t_0))$

k	1	2	3	4	5	6	7	8	9	10	11
$n_k(t_0)$	8025	605	129	41	16	8	4	2	1	1	1
Est under \mathcal{F}_2	8027.6	586.8	141.9	46.3	17.4	7.2	3.1	1.4	0.7	0.3	0.2

likelihood method fits the intensity function to the 1-appearance times, while the curve fitting method fits the corresponding cumulative function to cumulated data.

7 Swine feces data – a data with suspected zero-probability species

Consider the data for the pooled contig spectra from seven non-medicated swine feces. The data which are presented in Table 1, are studied in Chiu and Chao [2016].

The large $n_1(t_0)$ relative to other frequencies is interpreted as a signal for sequencing errors. Chiu and Chao [2016] proposes replacing the raw singleton count by a nonparametric singleton count estimate, and proceeds as if the adjusted value is real.

The belief that only the singleton count is unreliable can be interpreted as the singleton count is inflated by zero-probability species. Without loss of generality, we set $t_0 = 1$. To check whether $\nu(\{0\})$ is zero or not, we draw D2/D3 and D1/D2 plots in Fig. 2. The almost linear pattern in both plots indicates that both \mathcal{F}_1 and \mathcal{F}_2 are reasonable models. The intercept and slope of an approximate line in D1/D2 plot are 2.9 and 3.8 respectively, and those in D2/D3 plot are 0.5 and 1.1 respectively. The slope in D2/D3 plot lies outside the feasible range which is $[0, 1)$. Therefore, the maximum likelihood estimate may lie in the boundary of the feasible region. To check the above observations, we fit \mathcal{F}_2 , which is a mixture of zero-probability species and \mathcal{F}_1 to the data using the idea in the remark in Section 3. The estimated $\psi(t)$ is

$$\hat{\psi}(t) = 8028(0t + \mathcal{F}_1(t \mid 1, 2.878, 3.963)).$$

The first parameter for \mathcal{F}_1 , which is a scale parameter is fixed to one. The second and third parameters are close to the intercept and slope of an approximate line in D1/D2 plot respectively. The estimated weight for the zero-probability species is 0, which is in

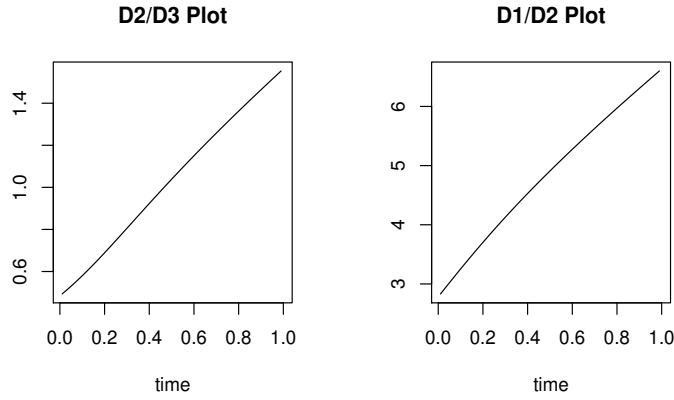


Figure 2: D2/D3 plot and D1/D2 plot for the swine feces data. As $\mathcal{F}_1 \subset \mathcal{F}_2$, approximate linear curve in D1/D2 plot usually accompanies with approximate linear curve in D2/D3 plot. Likelihood ratio test can be used to determine which model to use.

the boundary of the feasible region. The estimated $E(N_k(t_0))$ for various k are listed in Table 1. As the estimated c for \mathcal{F}_1 is larger than 1, the estimated D is infinite.

8 Conclusion

The contributions of this paper are summarized as follows.

First, we introduce a general framework, called the mixed Poisson partition process which is parameterized by a species intensity measure on the non-negative half real-line. The number of species can be finite or infinite. The expected number of individuals seen in any finite time interval can be infinite, and there can be infinite number of species with zero detection probability.

Second, in the proposed framework, we can specify a model using an expected species accumulation curve, or a species abundance distribution and $E(N_+(t_0))$ as a whole. The expected species accumulation curve can be any Bernstein function that passes through the origin. Maximum likelihood method can be applied whenever such a curve is given.

Third, we introduce two families of expected species accumulation curve, \mathcal{F}_1 and \mathcal{F}_2 . It includes and provides new insight to the power law. Associated with the families, we propose 1/D1 plot, D1/D2 plot, D2/D3 plot and log(D)-log plot which are simple

and informative graphical tools in discovering the latent structure of the data.

Fourth, we consider sampling design other than fixing the study period. A simple alternative is to fix the number of observed species. The ρ -appearance design puts more effort on rare species than common species. In this design, we need to balance the information loss and the amount of labor saved in recording common species. A simple example in Appendix E shows that the loss when $\rho = 4$ is minor. More studies are needed to explore the value of this design.

References

I. Abnizova, R. te Boekhorst, and Y. Orlov. Computational errors and biases in short read next generation sequencing. *J Proteomics Bioinform*, 10(1):1–17, 2017.

O. Arrhenius. Species and area. *Journal of Ecology*, 9(1):95–99, 1921.

J. Béguinot. Extrapolation of the species accumulation curve associated to “chao” estimator of the number of unrecorded species: a mathematically consistent derivation. 2016.

J. O. Berger and D. A. Berry. The relevance of stopping rules in statistical inference. *Statistical decision theory and related topics IV*, 1:29–47, 1988.

S. Bernstein. Sur les fonctions absolument monotones. *Acta Mathematica*, 52:1–66, 1929.

S. Boneh, A. Boneh, and R. J. Caron. Estimating the prediction function and the number of unseen species in sampling with replacement. *Journal of the American Statistical Association*, 93(441):372–379, 1998.

C.-H. Chiu and A. Chao. Estimating and comparing microbial diversity in the presence of sequencing errors. *PeerJ*, 4:e1634, 2016.

R. K. Colwell, A. Chao, N. J. Gotelli, S.-Y. Lin, C. X. Mao, R. L. Chazdon, and J. T. Longino. Models and estimators linking individual-based and sample-based rarefaction, extrapolation and comparison of assemblages. *Journal of plant ecology*, 5(1):3–21, 2012.

J. Dengler. Which function describes the species-area relationship best? a review and empirical evaluation. *Journal of Biogeography*, 36(4):728–744, 2009.

I. A. Dickie. Insidious effects of sequencing errors on perceived diversity in molecular surveys. *The New Phytologist*, 188(4):916–918, 2010.

S. Engen. On species frequency models. *Biometrika*, 61(2):263–270, 1974.

R. Fisher, A. Corbet, and C. Williams. The relation between the number of species and the number of individuals in a random sample of an animal population. *Journal of Animal Ecology*, 12:42–58, 1943.

I. Good and G. Toulmin. The number of new species, and the increase in population coverage, when a sample is increased. *Biometrika*, 43(1-2):45–63, 1956.

J. F. C. Kingman. *Poisson Processes*. Oxford University Press, 1993.

S. Kobayashi. The species-area relation ii. a second model for continuous sampling. *Researches on Population Ecology*, 16(2):265–280, 1975.

A. E. Magurran. Species abundance distributions over time. *Ecology letters*, 10(5):347–354, 2007.

T. J. Matthews and R. J. Whittaker. Fitting and comparing competing models of the species abundance distribution: assessment and prospect. *Frontiers of Biogeography*, 6(2), 2014.

T. J. Matthews and R. J. Whittaker. On the species abundance distribution in applied ecology and biodiversity management. *Journal of Applied Ecology*, 52(2):443–454, 2015.

R. M. May. Patterns of species abundance and diversity. *Ecology and evolution of communities*, pages 81–120, 1975.

B. J. McGill, R. S. Etienne, J. S. Gray, D. Alonso, M. J. Anderson, H. K. Benecha, M. Dornelas, B. J. Enquist, J. L. Green, F. He, et al. Species abundance distributions: moving beyond single prediction theories to integration within an ecological framework. *Ecology letters*, 10(10):995–1015, 2007.

J. L. Norris and K. H. Pollock. Non-parametric MLE for Poisson species abundance models allowing for heterogeneity between species. *Environmental and Ecological Statistics*, 5(4):391–402, 1998.

F. Preston. Time and space and the variation of species. *Ecology*, 41(4):612–627, 1960.

C. Quince, A. Lanzen, R. J. Davenport, and P. J. Turnbaugh. Removing noise from pyrosequenced amplicons. *BMC bioinformatics*, 12(1):38, 2011.

H. Raiffa and R. Schlaifer. Applied statistical decision theory. 1961.

R. L. Schilling, R. Song, and Z. Vondracek. *Bernstein functions: theory and applications*, volume 37. Walter de Gruyter, 2012.

E. Tjørve. Shapes and functions of species-area curves: a review of possible models. *Journal of Biogeography*, 30:827–835, 2003.

E. Tjørve. Shapes and functions of species-area curves (ii): a review of new models and parameterizations. *Journal of Biogeography*, 36:1435–1445, 2009.

E. P. White, P. B. Adler, W. K. Lauenroth, R. A. Gill, D. Greenberg, K. D. M, A. Rassweiler, J. A. Rusak, M. S. Smith, J. R. Steinbeck, R. B. Waide, and Y. Yao. A comparison of the species–time relationship across ecosystems and taxonomic groups. *Oikos*, 112(1):185–195, 2006.

M. Zhou, S. Favaro, and S. G. Walker. Frequency of frequencies distributions and size-dependent exchangeable random partitions. *Journal of the American Statistical Association*, 112(520):1623–1635, 2017.

Appendix A: Proof of the equivalence of the two definitions of the mixed Poisson partition process

The equivalence between the two definitions is a direct consequence of the marking theorem of Poisson process Kingman [1993]. Consider the joint process $\{(\lambda_i, t_i)\}$ in Definition 1 for $\lambda > 0$, where t_i is the first point of η_i . By the marking theorem, this process is a Poisson process with intensity measure $\lambda e^{-\lambda t} \tilde{\nu} = e^{-\lambda t} \mathbf{1}\{\lambda > 0\} \nu$ (we write $f(\lambda, t)\nu$ for the measure $A \mapsto \int \int_0^\infty \mathbf{1}\{(\lambda, t) \in A\} f(\lambda, t)\nu(d\lambda)$), where $\mathbf{1}\{.\}$ is

the indicator function. Since η_0 is a Poisson process with rate $\nu(\{0\})$, its contribution to the process $\{(\lambda_i, t_i)\}$ has an intensity measure $\mathbf{1}\{\lambda = 0\}\nu$. By the superposition property of Poisson process, the overall intensity measure of the $\{(\lambda_i, t_i)\}$ process is $e^{-\lambda t}\mathbf{1}\{\lambda > 0\}\nu + \mathbf{1}\{\lambda = 0\}\nu = e^{-\lambda t}\nu$.

Appendix B: Proof of the nested structure among $\{\mathcal{F}_j\}$

For positive integer j , $\mathcal{F}_j \subset \mathcal{F}_{j+1}$ holds because $-\psi^{(j)}(t) = (b + ct)\psi^{(j+1)}(t)$ implies $-\psi^{(j+1)}(t) = c\psi^{(j+1)}(t) + (b + ct)\psi^{(j+2)}(t)$. The fact that $\mathcal{F}_1 \neq \mathcal{F}_2$ is proved in Section 5.2. We need only to show that $\mathcal{F}_2 = \mathcal{F}_3 = \dots$. For any species accumulation curve $\psi(t)$, define $\phi(t) = \psi^{(1)}(0) - \psi^{(1)}(t)$. Clearly for $j = 1, 2, \dots$

$$\phi(t) \in \mathcal{F}_j \text{ if and only if } \psi(t) \in \mathcal{F}_{j+1}. \quad (23)$$

Suppose $\psi(t) \in \mathcal{F}_3$, say $-\psi^{(3)}(t)/\psi^{(4)}(t) = \tilde{b} + \tilde{c}t$. Then $\phi(t) \in \mathcal{F}_2$ and $-\phi^{(2)}(t)/\phi^{(3)}(t) = \tilde{b} + \tilde{c}t$. From the result in Section 5.2,

$$\phi(t) = \tilde{r}t + \mathcal{F}_1(t \mid \tilde{a}(\tilde{b} + \tilde{c})/(1 - \tilde{c}), \tilde{b}/(1 - \tilde{c}), \tilde{c}/(1 - \tilde{c})), \quad (24)$$

for $0 \leq \tilde{c} < 1$ and $\tilde{r} \geq 0$. Thus the general form of $\psi(t)$ which relates to the integration of $-\phi(t)$ has a term $-\tilde{r}t^2/2$. As $\psi(t)$ is a Bernstein function, the power of t cannot be larger than one. It implies that \tilde{r} must be zero. From (24), $\phi(t) \in \mathcal{F}_1$. From (23), $\psi \in \mathcal{F}_2$. It proves

$$\mathcal{F}_3 = \mathcal{F}_2. \quad (25)$$

Let $\psi(t) \in \mathcal{F}_4$. From (23), $\phi(t) \in \mathcal{F}_3$. From (25), $\phi(t) \in \mathcal{F}_2$. From (23), $\psi(t) \in \mathcal{F}_3$. Thus $\mathcal{F}_4 = \mathcal{F}_3$. Similarly, we can show $\mathcal{F}_5 = \mathcal{F}_4$. Repeating the same procedure, we prove $\mathcal{F}_2 = \mathcal{F}_3 = \dots$ by mathematical induction.

Appendix C: Proof of the fact that power law is the only law with time-invariant species abundance distribution

Suppose $p(t) = p = (p_1, p_2, \dots)$ which does not depend on t . For $k = 1, 2, \dots$,

$$p_k \psi(t) = E(N_k(t)) = \int \frac{\exp(-\lambda t) \lambda^{k-1} t^k}{k!} \nu(d\lambda).$$

Therefore, for any y ,

$$\left(\sum_{k=1}^{\infty} p_k (1-y)^k \right) \psi(t) = \int \frac{\exp(-\lambda t)}{\lambda} \sum_{k=1}^{\infty} \frac{((1-y)\lambda t)^k}{k!} \nu(d\lambda) = \psi(t) - \psi(yt).$$

It follows that

$$\psi(yt) = \psi(t) \left(1 - \sum_{k=1}^{\infty} p_k (1-y)^k \right).$$

Take logarithm on both sides, take derivative with respect to t , and then set $t = 1$. We have

$$y\psi^{(1)}(y) = \frac{\psi^{(1)}(1)\psi(y)}{\psi(1)}.$$

The solution of the above differential equation is $\psi(y) = \psi(1)y^{\psi^{(1)}(1)/\psi(1)}$ which is the power law. Hence the power law is the only law with $p(t)$ independent on t .

Appendix D: Direct proof of the log-likelihood function for ρ -appearance design

For a species with rate λ , the probability function of J is

$$pr(J = j \mid \lambda) = \begin{cases} \frac{(\lambda t_0)^j e^{-\lambda t_0}}{j!} & (j < \rho) \\ \sum_{k=\rho}^{\infty} \frac{(\lambda t_0)^k e^{-\lambda t_0}}{k!} & (j = \rho). \end{cases} \quad (26)$$

Since the time of the ρ th individual follows Erlang(ρ, λ),

$$pr(R \in [r, r + dr), J = \rho \mid \lambda) = \frac{\lambda^\rho r^{\rho-1} e^{-\lambda r}}{(\rho-1)!} dr. \quad (27)$$

By (26) and (27), the joint probability density function of the observations $\{(R_i, J_i)\}_{i \leq n_+(t_0)}$ given ν is proportional to

$$e^{-\psi(t_0)} \left(\prod_{i: j_i < \rho} \int \frac{\lambda^{j_i-1} t_0^{j_i} e^{-\lambda t_0}}{j_i!} \nu(d\lambda) \right) \left(\prod_{i: j_i = \rho} \int \frac{\lambda^{\rho-1} r_i^{\rho-1} e^{-\lambda r_i}}{(\rho-1)!} \nu(d\lambda) \right).$$

Therefore, the log-likelihood function is

$$\log(\mathcal{L}(\nu \mid \{r_i, j_i\}_i)) = -\psi(t_0) + \sum_{j=1}^{\rho-1} n_j(t_0) \log(\mid \psi^{(j)}(t_0) \mid) + \sum_{r_i < t_0} \log(\mid \psi^{(\rho)}(r_i) \mid).$$

Appendix E: Small simulation experiment on the loss of information of the ρ -appearance design

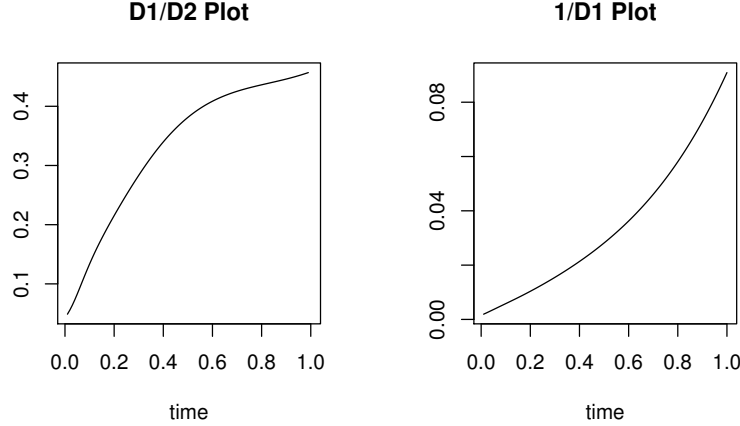


Figure 3: D1/D2 plot and 1/D1 plot for the Wisconsin route of the North American breeding bird survey data, 1995

0,0,0,0,0,0,1,1). Totally 645 birds from 72 species are recorded. The left panel in Fig. 3 shows the D1/D2 plot of the data. Clearly \mathcal{F}_1 does not fit the data well. The convex curve in the 1/D1 plot in the right panel indicates that D is finite. Let us consider $\nu(d\lambda) = \gamma f(\lambda | \mu, \sigma)d\lambda$ where $f(\lambda | \mu, \sigma)$ is the density function of $\text{Lognormal}(\mu, \sigma^2)$ distribution. The parameter γ is the expected total number of species. From Section 3, the maximum likelihood estimate of μ and σ is identical to the conditional maximum likelihood estimate of the corresponding Poisson-lognormal model. The fitted lognormal mixing distribution is $\text{Lognormal}(\hat{\mu}, \hat{\sigma}^2)$ distribution with $\hat{\mu} = 1.23$ and $\hat{\sigma} = 1.30$. Let $\varphi_i(\mu, \sigma) = \text{pr}(Y = i)$ where Y is a Poisson-lognormal random variable with parameters μ and σ . We use the function “dpoilog” of R-package “poilog” to compute this probability. The estimated γ is $\hat{\gamma} = n_+(t_0)/(1 - \varphi_0(\hat{\mu}, \hat{\sigma}^2)) = 85.2$.

Without loss of generality, set $t_0 = 1$. We use this data to investigate the information loss of the ρ -appearance design. The ρ -appearance data are simulated from the data using the following procedure:

Simulation procedure: Suppose species i has observed frequency m_i in time $[0, 1]$. If $m_i < \rho$, our data for this species is m_i , the frequency of it in time $[0, 1]$. If $m_i \geq \rho$, we simulate the ρ -appearance time of the species, r_i from $\text{Beta}(\rho, m_i + 1 - \rho)$ distribution, which is the distribution of the ρ order statistic of m_i samples from the $U(0, 1)$ distribution.

It can be shown that $E(N_k(t)) = \gamma\varphi_k(\mu + \log(t), \sigma)$. The log-likelihood function is

$$\begin{aligned} & \log(\mathcal{L}(\gamma, \mu, \sigma \mid \{r_i, j_i\}_i)) \\ = & -\gamma(1 - \varphi_0(\mu, \sigma)) + \sum_{k=1}^{\rho-1} n_k(1) \log(\gamma\varphi_k(\mu, \sigma)) + \sum_{r_i < 1} \log(\gamma\varphi_\rho(\mu + \log(r_i), \sigma)). \end{aligned}$$

The maximum likelihood estimate for $E(N_+(1)) = \gamma(1 - \varphi_0(\mu, \sigma))$ is $n_+(1)$. The function that we need to maximize to find $\hat{\mu}$ and $\hat{\sigma}$ is

$$h(\mu, \sigma) = -n_+(1) \log(1 - \varphi_0(\mu, \sigma)) + \sum_{k=1}^{\rho-1} n_k(1) \log(\varphi_k(\mu, \sigma)) + \sum_{r_i < 1} \log(\varphi_\rho(\mu + \log(r_i), \sigma)).$$

The maximum likelihood estimate of γ is $\hat{\gamma} = n_+(1)/(1 - \varphi_0(\hat{\mu}, \hat{\sigma}))$. We consider $\rho = 1, 2, \dots, 6$. For each ρ -value, we simulate 100 independent sets of ρ -appearance data. For each simulated data, μ , σ and γ are estimated. The sample mean and sample standard deviation of the estimates are presented in Table A. Graphical display is given in Fig. 4.

The mean of the estimate is close to that basing on $\tilde{n}(t_0)$. The standard deviation of the estimator decreases as ρ increases. We should avoid choosing $\rho = 1$, which is significantly inferior to $\rho = 2$. The effect of ρ on the standard deviation varies across parameters. Value $\rho = 4$ performs well for this data. The total number of species with frequency less than 4 is 33, around 46% of the seen species, and total number of individuals is 65, around 10% of the total number of individuals detected. If 4-appearance design is used, we need only to record about 10% of all seen individuals.

Table A. Mean and standard deviation of estimators for North American breeding

ρ	bird survey data (1995)						
	1	2	3	4	5	6	∞
mean of $\hat{\mu}$	1.10	1.28	1.23	1.21	1.21	1.22	1.23
sd of $\hat{\mu}$	0.56	0.09	0.07	0.04	0.04	0.03	0*
mean of $\hat{\sigma}$	1.39	1.24	1.29	1.29	1.31	1.30	1.30
sd of $\hat{\sigma}$	0.48	0.15	0.13	0.08	0.09	0.07	0*
mean of $\hat{\gamma}$	90.4	83.8	85.0	85.5	85.7	85.3	85.2
sd of $\hat{\gamma}$	18.7	2.52	2.32	1.38	1.56	1.29	0*

* When $\rho = \infty$, we always observe the full data, and the sample standard deviation (sd) of the estimator across simulation is zero.

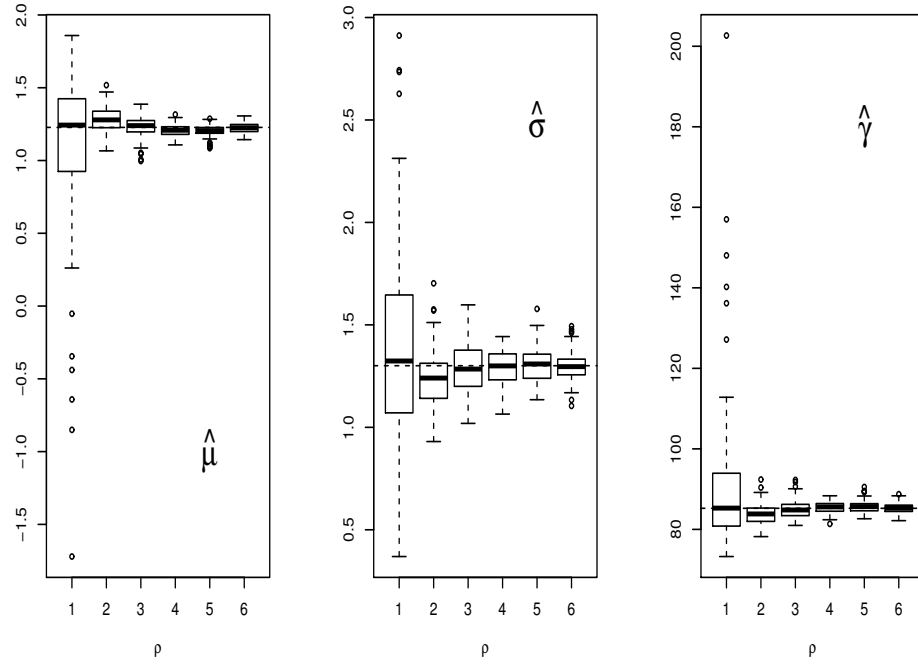


Figure 4: Box-and-whisker plots for estimators across different values of ρ in the simulation. The horizontal dashed line in each plot shows the estimate when the full Wisconsin route of the North American breeding bird survey data for 1995 is used. The variability in the estimate delineates the additional noise due to the ρ -appearance design.